Proceedings of the ASME 2018
International Mechanical Engineering Congress and Exposition
IMECE2018
November 9-15, 2018, Pittsburgh, PA, USA

IMECE2018-87008

EFFECT OF DIFFERENT CUTTING DEPTHS TO THE CUTTING FORCES AND MACHINING QUALITY OF CFRP PARTS IN ORTHOGONAL CUTTING – A NUMERICAL AND EXPERIMENTAL COMPARISON

Farid MIAH[1], Emmanuel DE-LUYCKER[2], Frederic LACHAUD[1], Yann LANDON[1], Robert PIQUET[1]

[1]Institut Clément Ader (ICA), Université de Toulouse, CNRS, INSA, ISAE-SUPAERO, Mines Albi, UPS, Toulouse, France
[2]Laboratoire Génie de Production, LGP, Université de Toulouse, INP-ENIT, Tarbes, France

ABSTRACT

The necessity of understanding the influence of cutting variables in orthogonal cutting of Carbon Fiber Reinforced Polymer (CFRP) is vital because of their significant influences to the quality of manufactured parts. In this present research work the influences of different cutting depths to the cutting and thrust forces have been analyzed and a comparison between an equivalent homogeneous material (EHM) macro-model and experimental results have been made. The reasons of the beginning high cutting and thrust forces have been studied and explained. The post analysis of the experimental machined surfaces has been done to analyze the generated surface roughness and fiber-matrix interface crack generation. Five different cutting depths and four individual fiber orientations have been tested both numerically and experimentally. Significant influence of cutting depths to the cutting force has been found and the surface quality of newly generated machined part is discovered as a function of cutting depth and fiber orientation.

INTRODUCTION

Because of the high mechanical strength with respect to the density, good resistance to corrosion and to fatigue, composite materials can play an important role to the aeronautic and automotive structures. Nowadays, the extension use of composite structures in aeronautics and automotive is raising many complications in the manufacturing processes, including orthogonal cutting process as these materials contain multiple phases. Orthogonal cutting is a type of material cutting technique in which the cutting tool generates a plane surface which is parallel to the original planar surface of the machined material [Merchant, 1945]. This surface is machined with a cutting edge perpendicular to the direction of the relative displacement between the tool and the workpiece.

Recently the research activities in orthogonal cutting of composite laminates have been increased indeed the numerical modeling of composite cutting is still poorly developed [Cantero et al. 2012]. According to [Lasri et al., 2009], the machining of fiber reinforced polymer (FRP) materials differs from machining conventional metals and their alloys due to the heterogeneity and anisotropy of FRP materials. [Liu et al., 2012] noted that composite laminates are regarded as hard-to-machine materials, because of low machining efficiency and undesirable machining-induced delamination. But the simple condition of orthogonal machining in studying chip formation permits to gather knowledge about different components like chip shape and size, shear stress and strain in the chip, friction conditions, cutting forces, cutting temperatures, etc. [Klinkova et al., 2011].

Regarding the orthogonal cutting of Carbon Fiber Reinforced Polymer (CFRP) many answers in literature are limited, especially concerning how different cutting depths affect the cutting and thrust forces and the machining quality of manufactured parts. On the subject of cutting depth influence [Zitoune et al. 2005] analyzed the cutting forces using 0.05 to 0.25mm cutting depth and 0°, 45°, 90° and 135° fiber orientation of unidirectional T2H/EH25 materials . In their numerical model only 0° fiber orientation has been used. However, their research does not talk about the thrust forces and the effect of a cutting depth greater than 0.25mm. [Blanchet, 2015] analyzed the resultant force of F_c (cutting force) and F_t (thrust force) and the machined surface quality with respect to the cutting speed from quasi-static to 120 m/min. He used four different fiber orientations but kept the cutting depth constant throughout the whole research. [Wang and Zhang, 2003] focused on the machining forces with respect to the rake angle and fiber orientation but in their research the maximum cutting depth used was 0.25 mm which does not disclose the influence of higher cutting depth. Several analytical models [Bhatnagar et al., 1995] [Zhang et al., 2001] [Jahromi and Bahr, 2010] have been found to predict the cutting forces but the concern of cutting depth's affect is missing. The numerical models mentioned here to predict the cutting and thrust forces mainly used an equivalent homogeneous material (EHM) which, basically, deviate the numerical result from experimentation. [Nayak et al., 2005] tried to amend it by modeling the fiber and matrix separately without taking matrix damage in calculating the cutting forces. It was found that both the cutting and thrust forces matched quite well with the experimental results.

In this present research work a comparison between numerical (Finite Element Analysis) and experimental research have been carried out on the influences of different cutting depth to the cutting and thrust forces, surface roughness, subsurface damage and fiber-matrix interface debonding. Five different cutting depths (0.1mm, 0.25mm, 0.50mm, 0.75mm and 1.0 mm) and four different fiber orientations (0°, 45°, 90° and 135°) have been used in orthogonal cutting of CFRP both numerically and experimentally. Each cutting depth has been tested with four fiber orientations while the cutting speed was kept constant during all tests. The cutting force and thrust force have been analyzed for every cutting depth and fiber orientations.

Since the machined surface quality and subsurface damage have been known to be highly dependent on many process parameters, there have been many previous studies focused separately on the effect of fiber position, cutting speed, rake angle on the surface quality, eg: [Blanchet, 2015] [Iliescu, 2008][Shchurov et al., 2016] [Arola et al., 1996] [Arola et al., 2002] [Alaiji et al., 2015] [Wang and Zhang, 2003]. Different failure models, Hashin, Maximum stress and Hoffman criterion have been used by [Lasri et al., 2009] focusing on progressive failure of unidirectional glass fiber-reinforced polymer composite (FRP). The outputs answered many questions regarding the machining surface quality; nevertheless, the effect of different cutting depth is not answered yet. The present research carried out a post analysis of newly generated machined surfaces to analyze the surface roughness and crack generation and propagation in the fiber-matrix interface as function of cutting depth. Simultaneously, the work also shows in-depth findings regarding the influence of fiber orientation to the surface quality of machined part.

Initially, once the tool touches the workpiece the cutting and thrust force get higher and become unstable which later decreases and stabilized. Any analytical description of this phenomenon has not been found in the literature. In this research work the reason of this initial high force has been analyzed and explained.

It has been found both numerically and experimentally that the cutting force increases if the cutting depth increases but the thrust force varies mostly depending on fiber orientations. Surface quality and fiber-matrix interfacial crack of machined part mostly depends on the fiber orientation rather than cutting depth.

NUMERICAL MODEL

Geometry and Boundary Conditions

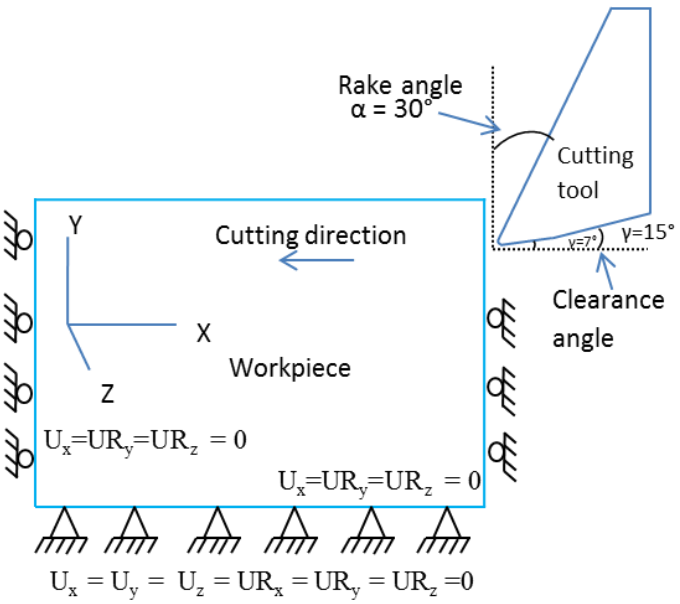

Fig.1. Schematic 2D view of numerical model.

A three-dimensional (3D) finite element (FE) model has been developed to analyze the machining forces and cutting induced damages on the machined surface. The workpiece has been modeled as a 3D deformable solid part. The bottom of the rectangular workpiece has been fixed by considering $U_x = U_y =$

$U_z = UR_x = UR_y = UR_z = 0$; the displacement and rotation in X (cutting direction) and Z (transverse direction) directions have been blocked by $U_x=UR_y=UR_z=0$ and $U_z=UR_x=UR_y=0$ respectively as in Fig.1. The cutting tool has been modeled as a discrete rigid shell part. The rake and clearance angles, $\alpha = 30°$, $\gamma = 7°$ and 15°; have been used in all simulations. Two different clearance angles have been used at the same time (7° near the tool tip and 15° at the end) following the experimental cutting tool's geometry. The displacement freedom of cutting tool has remained in X direction by $U_y=U_z=UR_x=UR_y = UR_z = 0$ whereas a reference point is used to control the movement.

Contact Modeling

It should be noted that in numerical model it is very difficult to simulate ideal friction behavior. In this model a penalty friction formulation with friction coefficient 0.3 has been used following Coulomb friction model, Eq. 1, to define the interaction between the cutting tool and the workpiece. It permits some relative motion; i.e. elastic slip, of the actual surface when they should remain sticking.

$$\tau_{lim} = \mu P + b \tag{1}$$

$$|\tau| \leq \tau_{lim} \tag{2}$$

Here τ_{lim} is the limiting shear stress, τ is the equivalent shear stress, μ, P *and* b are the friction coefficient, contact pressure and cohesion sliding resistance with zero normal pressure respectively.

Material and Failure Criteria

An equivalent homogeneous anisotropic material has been used to predict the machining forces. Both the fiber and matrix materials are assumed to be isotropic. By using the homogenization procedure and the FEM, the global constitutive behavior of the corresponding orthotropic material has been framed by symmetric stiffness matrix. C3D8R 8-node linear brick hexagonal elements with reduced integration has been used for the workpiece throughout the simulations. The cinematic split has been controlled by the average strain. 4 node 3D bilinear rigid quadrilateral elements, R3D4, has been used for cutting tool.

The failure modes have been managed by a Continum Damage Mechanics (CDM) type constitutive law, which was first developed by [Matzenmiller, 1995] and later modified by [Ilyas, 2010] and [Blanchet, 2015]. From the different modes of rupture 5 damage criteria have been defined; 1-tensile failure criterion in fiber direction, 2-compressive failure criterion in fiber direction, 3-matrix crushing criteria, 4-matrix failure criteria and 5-delamination damage criteria. This constitutive law was integrated by a VUMAT sub-routine.

Adaptive Mashing and Distortion Control

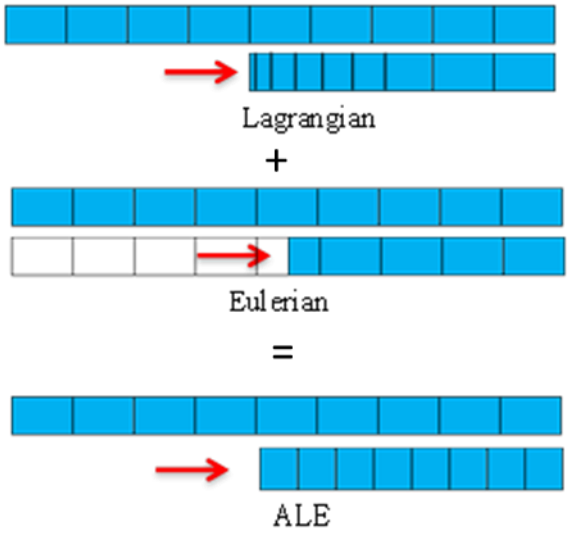

Fig.2. Arbitrary Lagrangian-Eulerian (ALE) method.

Arbitrary Lagrangian-Eulerian (ALE) adaptive meshing has been used to retain high-quality mesh by maintaining large deformations and losses of material throughout the analysis. ALE combines the features of pure Lagrangian analysis and pure Eulerian analysis [Abaqus User Manuel, 2016] Fig. 2. It allows the nodes to move while the topology remains unchanged according to the Eq.3.

$$\mathrm{X}_{i+1} = \mathrm{X} + u_{i+1} = \mathrm{N}^N \mathrm{x}_i^N \tag{3}$$

Here, X is the original position and X_{i+1} is the new position of a node, u_{i+1} its nodal displacement, x_i^N is neighboring nodal positions and N^N is weight functions.

The Frequency used was 10 with remeshing sweep per increment 6 and the boundary region smoothing has been used as default values which are 30 for initial feature angle, 30 for transition feature angle and 60 for mesh constraint angle.

EXPERIMENTAL CONFIGURATION

Machine Setup

The experimental configuration have been carried out with a single axis, quasi-static to 2m/sec cutting speed setup supported by a conventional milling machine, Fig. 3. The cutting tool is fixed and the workpiece is clamped in a movable device. The cutting speed is transmitted from a motor to the device containing the specimen via a ball screw module. The motor speed is computer controlled via a COMPAX 3 C3 S150 V4 F11 I12 T11 M00 case. A position sensor is integrated in the motor which allows recording the position and speed of the motor.

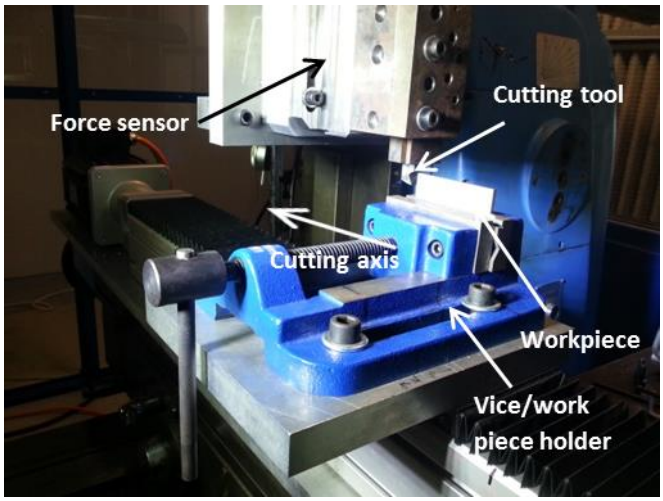

Fig.3. Experimental setup

The motor and the module for converting the rotational movement into translation movement are fixed on the table of the milling machine frame. The cutting tool is placed by a holder putting a KISLER 9257B triaxial force sensor in between the machine and the tool holder. The force sensor is tied to the fixed part of the milling machine by a chamber. The force sensor is designed to measure the forces in X, Y and Z directions where X represents the horizontal force (cutting force), Y represents the vertical force (thrust force) and Z represents the transverse force (e.g. reaction of vibration). Transverse force has not been taken into account as it is near zero for orthogonal cutting.

Materials and Cutting Conditions

An intermediate modulus unidirectional Carbon/Epoxy (T800S/M21) material has been used as a test specimen. Each specimen contains only one specific fiber orientation and 16 fiber layers. The Representative Elementary Volume (REV) of the workpiece is 80 mm * 4 mm * 45 mm. For the cutting tool, K20 micro grain tungsten carbide has been used. The cutting parameters have been shown in Tab.1.

Parameter	Values
Rake angle	30 degree
Clearance angle	7° and 15°
Depth of cut	0.1, 0.25, 0.50, 0.75 and 1.0 mm
Cutting speed	200 mm/sec (12 m/min)
Fiber and matrix volumetric ratio	60 % : 40 %
Fiber orientation	0°, 45°, 90°, and 135° separately
Frequency of force fluctuation	7000Hz/sec

Table.1. Cutting parameters.

Near the tool tip 7° clearance angle has been kept for 4 mm longer distance to maintain high stiffness to resist tip breaking. After this distance the angle is 15°.

RESULTS AND DISCUSSION

Cutting Force

In Fig.4. the cutting forces are separated according to fiber orientation and compared with respect to the cutting depths. It is clearly seen that there is a strong influence of cutting depths on the cutting forces. Regardless of fiber orientation, it is found that if the cutting depth increases, the cutting force increases as well both numerically and experimentally. At 0° fiber orientation, Fig.4 (a), the simulated force at every cutting depth is greater than the experimental forces whereas it is the contrary at 90° (Fig.4[c]) and 135° (Fig.4[d]) fiber angles. At 45° fiber orientation, Fig.4 (b), the experimental force gets higher at 0.5mm cutting depth. This result is comparable with [Alaiji et al., 2015] which found that if the fiber orientation is less than 40°, the experimental cutting force remains less than numerical value and if the orientation is more than 40° the experimental value gets higher than the numerical value. The reason for this phenomenon is because at 0° fiber orientation the tool needs comparably less force to complete the chip formation as the fibers are parallel to the cutting direction. Moreover, at this angle the fibers are not cut crosss-sectionally and there is minimum or no elastic return effect from the fiber. By the same token, at 135° fiber orientation, Fig. 135 (d), a large deviation between the numerical cutting force and experimental values is found indeed both forces have the same rising tendency with respect to the cutting depth. It is because at 135° fiber orientation the fibers are cut in big bunches rather than smooth cutting, causing an increase of the average cutting force. This phenomenon is less realistic in EHM model which is the cause of this deviation. Nevertheless, the trend of cutting forces predicted by FE simulations matched well with the experimental results.

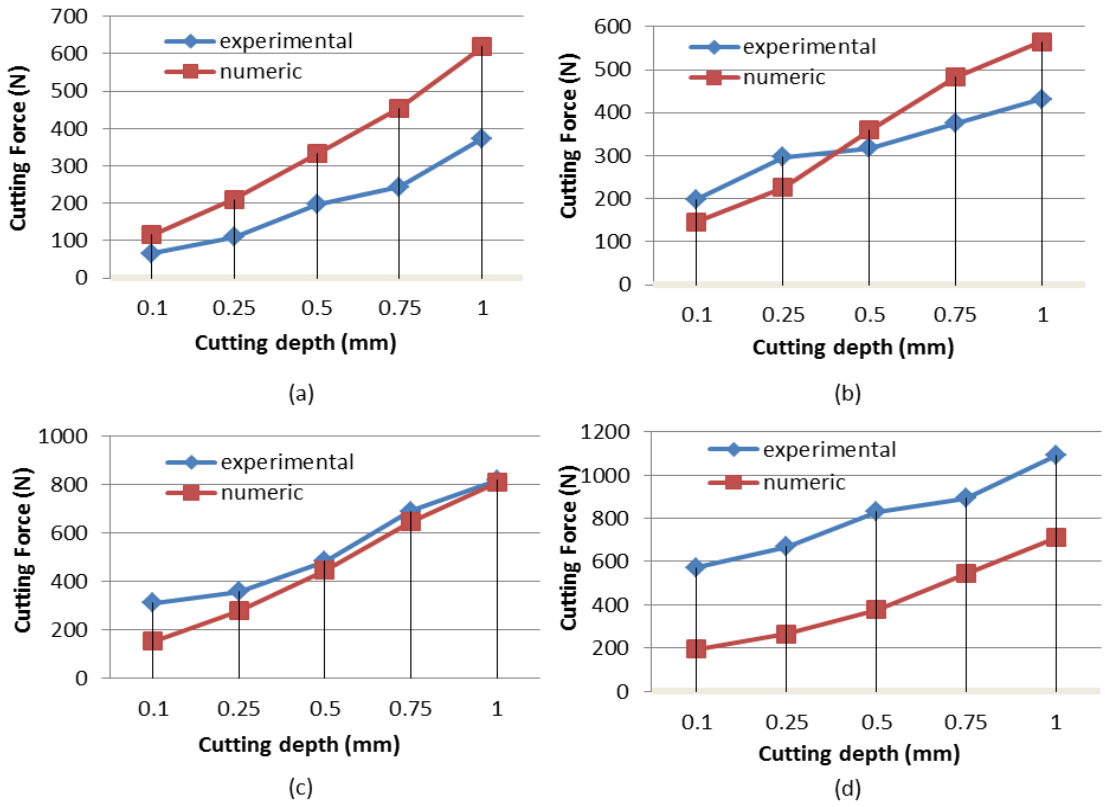

Fig.4. Comparison of numerical and experimental cutting forces: (a) 0° fiber orientation (b) 45° fiber orientation (c) 90° fiber orientation and (d) at 135° fiber orientation.

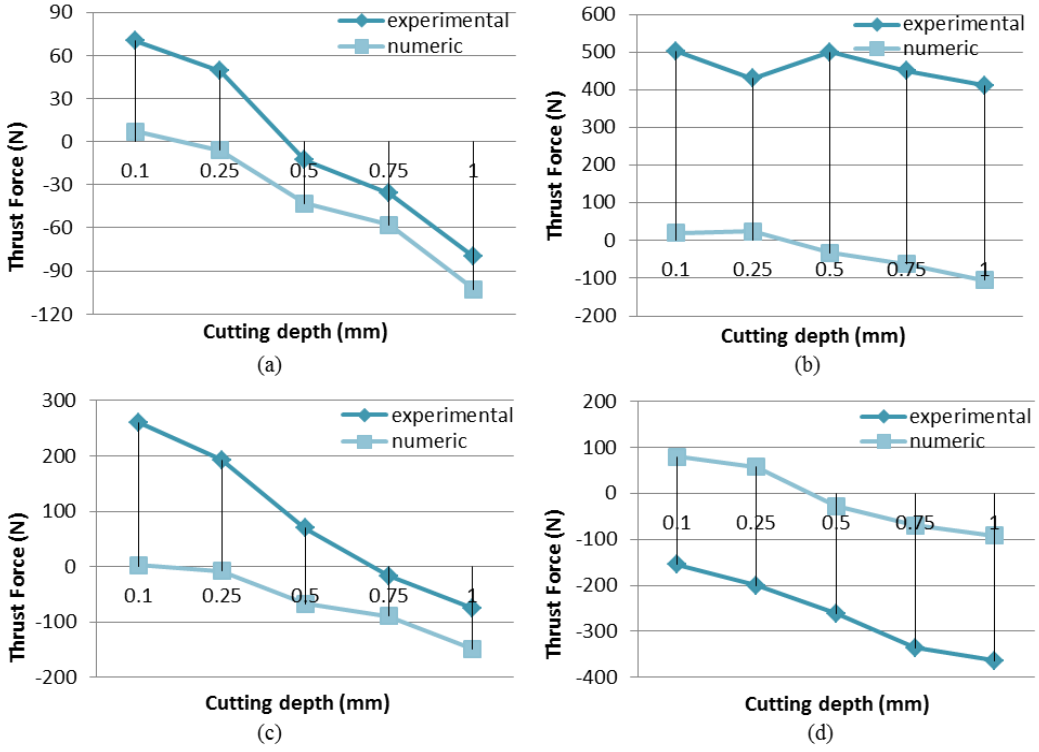

Fig.5. Comparison of numerical and experimental thrust forces: (a) 0° fiber orientation (b) 45° fiber orientation (c) 90° fiber orientation and (d) at 135° fiber orientation.

Thrust Force

By the recorded thrust force history, Fig. 5, it is learned that thrust force can be positive as well as negative depending on the cutting depth and fiber orientation (but cutting force stands always positive). It should be reported that thrust force strongly depends on the elastic return phenomenon; the same was found by [Lasri et al., 2009] and [Ghidossi et al., 2003]. Due to this phenomenon, the real and nominal depths of cut vary. Thrust force causes deflection of the tool and reduces the depth of cut and affects tolerances. But it fluctuates rapidly if the cutting depth is changed, and a small variation in experimental setup can change the result dramatically.

The thrust force drops if the cutting depth increases regardless of fiber orientation, which means it has inverse relationship with cutting depth. At 0.1mm cutting depth of 0° and 90° fiber position the thrust force is maximum seeing minimum at 1mm, Fig. 5 (a) and (c). For all cutting depths at 45° fiber orientation, Fig.5 (b), the experimental values remain always positive and at 135° orientation, Fig.5 (d), it is always negative. Additionally, a significant deviation between the numerical and experimental forces is found. The reason why is that, at 45° fiber orientation fiber experiences high downward pressing from the tool tip during cutting. Once the fiber is cut, due to elastic return characteristics it pushes upward on the clearance surface of the cutting tool more than any other fiber orientation. It is, as, at 45° fiber orientation that the fibers are inclined towards the cutting direction; consequently the clearance surface of the tool faces comparably more surface contact from the cross-sectional cut surface of fiber. More contact means more friction and high vertical force. On the other hand, at 135° fiber orientation the fibers are inclined at the opposite angle of cutting direction. Fiber does not face any downward pressing action from the tool tip and there is almost zero elastic return phenomenon. But as on the rake surface the tool faces downward vertical force from the ongoing cutting chip the total vertical force (thrust force) gets negative for all cutting depths. Here it should be remarked that according to the cutting mechanics, no matter how much the cutting depth is, at 45° fiber orientation the thrust force will always be positive and at 135° fiber orientation it will always be negative.

This particular thrust force phenomenon cannot be found by any HEM FEM model which is the fact in present research work too. The same cause was mentioned by [Gopala et al. 2007]. The HEM models found on literature are not realistic to represent the thrust force. To predict this phenomenon numerically the only way is to develop micro mechanical models with separate fiber and matrix properties. But it will not be easy as the model might have several hundreds of thousands of elements which may deserve large computer memory.

Eventually, it can be said that the trends of the predicted cutting and thrust forces at all cutting depths matched to the experimental results in spite of the fact that there are some deviations.

Force When the Tool Touches the Workpiece

It has been found that initially once the tool tip touches the workpiece the cutting force gets much higher and thrust force remains lower than the average value while both of the forces become unstable, Fig.6. These initial contact forces, induced due to the cutting tool, is a function of contact pressure, friction parameter and shear stress. While the tool touches the workpiece it faces a strong reaction force which lasts from initial tool-workpiece contact point to the initiation of fiber cut. This incident generates a momentary high vibration to the cutting tool and workpiece that affect the initial unstable contact forces. At the point of fibers separation (cut), the force reaches its peak values; once the front fibers start to be separated (cut), the force reduces until the total separation of the first chip (the first peak zones of the zoomed area of cutting and thrust forces of Fig.6.). The duration of this phenomenon was measured 0.0165 second (3.3mm cutting length at 200mm/sec cutting velocity) which is interestingly equal to the length of the first chip. Concurrently, the thrust force fluctuates both in positive and negative direction unstably; as in this very initial cutting zone, the fibers experience both pressing and cutting phenomenon. The same phenomenon is repeated during the course of the second chip generation (the second peak zones of the zoomed area of cutting and thrust forces of Fig.6.) though the second chip's length has been found around 4mm, longer than the first one. By the end of second chip separation (7.3mm total cut) the generated initial high vibration and instability in the tool and workpiece reduce considerably as both of them are held tightly in the holders.

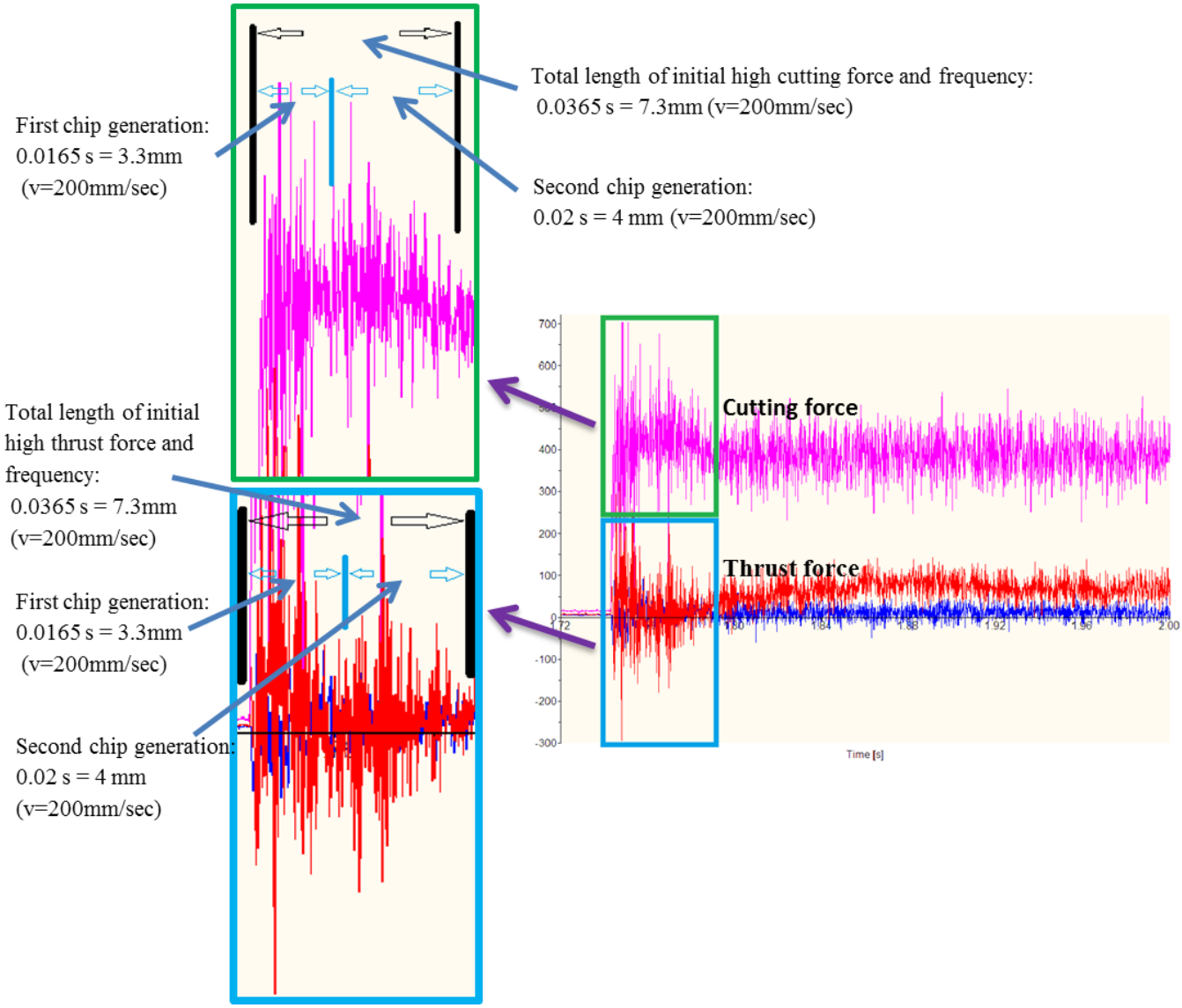

Fig.6. Initial contact forces (experimental).

SURFACE STATE

The quality of machined surface relies on many surface parameters. [Pramanik et al., 2007] mentioned that newly generated surfaces remain under residual compressive stress and these surfaces are damaged due to cavities left by the pull-out of fibers; whereas [Shchurov et al., 2016] said it is the interfacial debonding between fibers and matrix in the area under machined surface which is responsible. In this paper the surface roughness has been analyzed from experimental results following a numerical and experimental crack generation and propagation comparison.

Surface Roughness

In order to evaluate the surface roughness after machining, Alicona INFINITEFocus SL with standard straight edge 10x has been used. A cross-sectional measurement of the machined surface on the workpiece has been done taking a profile of 100 micrometer width. Typical surface profiles recorded for all cutting conditions. The parameter discussed here is mainly the

average roughness of the profile, R_a which if formulated according to the Eq.4.

$$R_a = \frac{1}{l}\int_0^1 |y(x)|dx \quad (4)$$

It is defined as the average absolute deviation of the roughness irregularities from the mean line over one sampling length as shown in Fig.7.

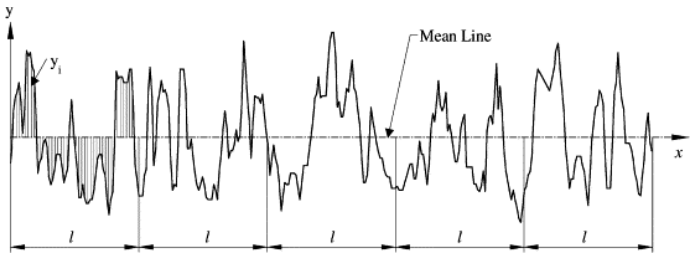

Fig.7. Arithmetic average height, R_a [Gadelmawla et al., 2002].

It has been found that the surface roughness height variation is dominated by the fiber orientation rather than the cutting depth.

At 0° fiber orientation, Fig. 8 (a), the average roughness remained from 0.33 µm to 0.38 µm while at 45° orientation, Fig.8 (b), it is always around 0.8 µm for all cutting depths. It should be noted that when the fibers are positioned at 0° they are parallel to the cutting direction; as a result they do not get cut cross-sectionally which gives smooth surface regardless of cutting depth. Comparably, at 45° fiber position the roughness is mainly generated by the elastic return of the fibers which previously get compressed by the tool tip during cutting. Consequently the roughness profile remains almost the same whatever the cutting depth. At 90° fiber orientation, Fig. 8 (c), there is little gradual increase of the roughness as the cutting depth increases; indeed, the maximum value does not pass over 2 µm. Two typical roughness profiles of 90° fiber angle can be seen at Fig.9.

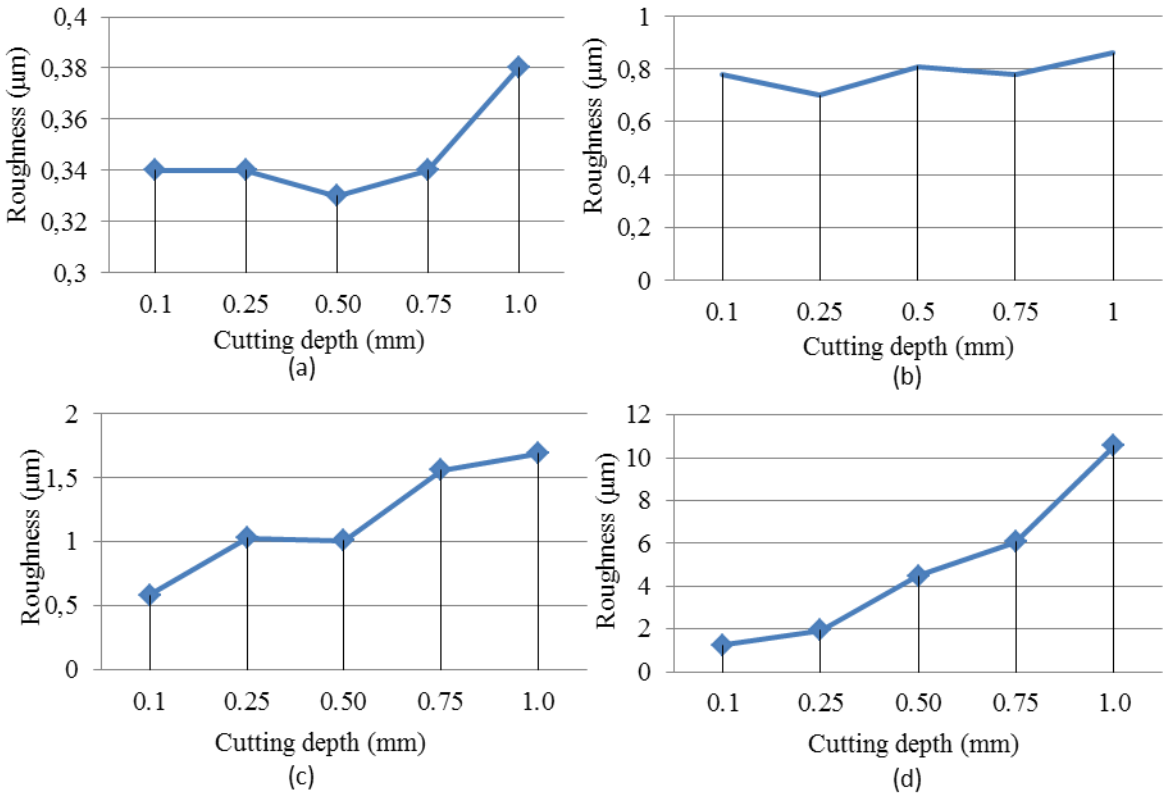

Fig.8. Roughness (experimental): (a) 0° fiber orientation (b) 45° fiber orientation (c) 90° fiber orientation and (d) at 135° fiber orientation.

A strong influence of cutting depth is seen at 135° fiber position, Fig.8 (d). As the fibers are inclined toward the opposite way of cutting direction, the apex of the cut surface of fibers get debonded from the matrix by the tool tip. Additionally, micro-cracks are generated along the fiber-matrix interface which gets longer depending on cutting depth. It is because the cross-sectional stiffness of fiber is higher than the adhesive force of the fiber-matrix interface. As a result, cracks are generated and propagated along the fiber-matrix interface. This argument well supports the findings of [Wang and Zhang, 2003] and [Koplev, 1983] which show that if the fiber orientation gets grater than 90°, the roughness increases rapidly, that means the fiber orientation plays an important role. Moreover, fibers are very abrasive which causes sharpness loss of cutting tool. The more the tool is used, the more it loses its sharpness, and, as a result, the radius of the tool tip increases, hence increased springback and surface roughness.

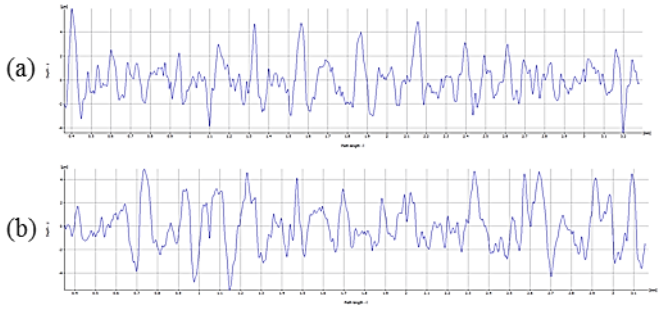

Fig.9. Typical roughness profile of 0.5 mm and 0.75 mm at 90° fiber orientation.

Crack Generation and Propagation

Subsurface damage or crack generation can be of different types according to [Lasri et al., 2009]; fiber-matrix interface debonding, inter-ply delamination, transverse matrix cracking and fiber rupture. The trend of rising crack and damage during cutting is found to be a function of cutting depth and fiber orientation. At 0° and 45° fiber position, at all cutting depths, no crack has been found, neither numerically nor experimentally. Thus the remarkable point is that the cutting depth has no influence on the surface damage at these fibers' positions. At 0.1 mm and 0.25 mm cutting depth of 90° fiber orientation no crack has been found experimentally indeed a number of cracks were seen numerically at 0.25 mm cutting depth. At 0.50 mm, 0.75 mm and 1 mm depth several noticeable cracks have been marked having 4mm long in experimentation and 2.1 mm in numerical model.

The significant crack generation and propagation have been found at 135° fiber orientation. A numerical and experimental comparison of generated cracks for different cutting depths is shown in Fig.10. On the figure it can be clearly seen that if the cutting depth increases, the crack extends. At 0.1 mm depth the fiber matrix interface crack is 0.85 mm in simulation and 4.5 mm in experimentation, whereas, at 1mm cutting depth the simulated crack is 10.2 mm and the experimental one is 14 mm. The simulated cracks are shorter than the experimental ones. The reason behind it is that in CFRP there are three different phases; fiber, matrix and fiber-matrix interface. Each of the phases contains distinct characteristics. As the cross-sectional stiffness of fiber is higher than the adhesive force between fiber and matrix, the fibers get debonded from the matrix which generates crack and permits to propagate depending on the amount of force exerted by the forwarding tool; similar note was found from [Shchurova et al., 2016]. Unlikely, the EHM model does not hold quietly those discrete characteristics which are the causes of varying result from experimentation.

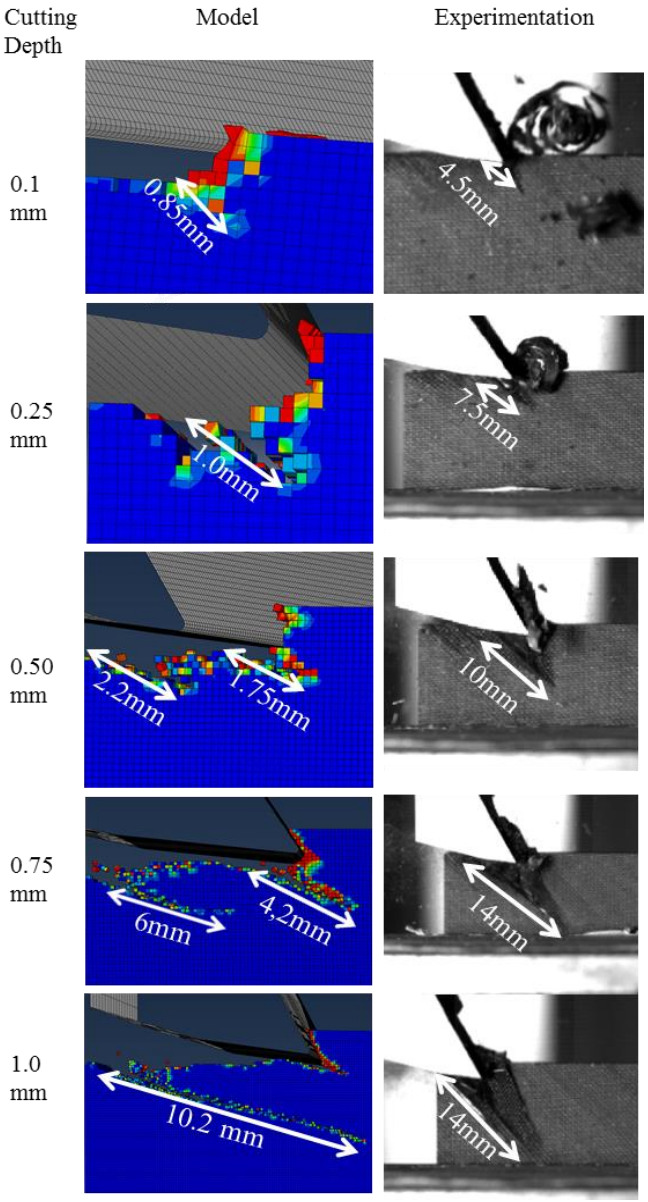

Fig.10. Numerical and experimental fiber-matrix interface crack as a function of cutting depth at 135° fiber position.

CONCLUSION

In orthogonal cutting depending on the type of material, the parts quality and generated defects can vary; and it is not because of the mechanics of cut but because of the individual characteristics of materials. Understanding the relationship of cutting variables with cutting quality and required cutting efforts is crucial to secure the best cutting parameters and to well understand their influences. A range of cutting depths has been used to analyze their influences to the machining forces and produced surface quality. The numerical results of cutting forces provide a good agreement with the experimental cutting forces, which reveals that the cutting force increases if the cutting depth increases; but the thrust force is mainly dominated by fiber orientation rather than cutting depths. Cutting depths has significant influence on surface roughness and crack generation principally at 90° and 135° fiber orientation. For any cutting depth at 135° fiber orientation the thrust force will always be negative (vertically downward) and at 45° fiber orientation always positive (vertically upward). The initial unstable high forces are functions of initial compression of fibers by the tool and generated vibration and instability in the cutting tool and the workpiece. This present work provides a framework for studying the cutting depths effects with micro-mechanical model later in future.

REFERENCES

Arola D., M. Ramulu, and D.H. Wang. 1996. “Chip Formation in Orthogonal Trimming of Graphite / epoxy Composite” 27 (2): 121–33.

Arola D., M. B. Sultan, and M. Ramulu. 2002. “Finite Element Modeling of Edge Trimming Fiber Reinforced Plastics.” Journal of Manufacturing Science and Engineering, 124 (1): 32–41.

Alaiji R. El., L. Lasri, and A. Bouayad. 2015. “3D Finite Element Modeling of Chip Formation and Induced Damage in Machining Fiber Reinforced Composites.” American Journal of Engineering Research (AJER) 4 (7): pp-123-132.

Bhatnagar, N., N. Ramakrishnan, Nk Naik, and R. Komanduri. 1995. “ON THE MACHINING OF FIBER-REINFORCED PLASTIC (FRP) COMPOSITE LAMINATES.” International Journal of Machine Tools & Manufacture, 35 (5), 701-716

Blanchet Florent. 2015. “Etude de la coupe en perçage par le biais d'essais élémentaires en coupe orthogonale : application aux composites carbone-époxy”. PhD Thesis, Université Toulouse 3–Paul Sabatier.

Cantero J. L., C. Santiuste, N. Marín, X. Soldani, H. Miguélez, Mariano Marcos, and Jorge Salguero. 2012. “2D and 3D Approaches to Simulation of Metal and Composite Cutting.” AIP Conference Proceedings 1431 (1): 651–59.

Ghidossi Patrick. 2003. Contribution à L’étude de L’effet des Conditions D’usinage D’éprouvettes en Composites à Matrice Polymère sur Leur Réponse Mécanique. PhD Thesis, ENSAM Paris.

Gopala Rao, G. Venu, P. Mahajan, and N. Bhatnagar. 2007. “Micro-Mechanical Modeling of Machining of FRP Composites – Cutting Force Analysis” 67 (3–4): 579–93.

Iliescu, Daniel. 2008. “Approches experimentale et numerique de l’usinage a sec des composites carbone /epoxy.” PhD Thesis, ENSAM PARIS.

Ilyas Muhammad. 2010. “Damage Modeling of Carbon Epoxy Laminated Composites Submitted to Impact Loading.” PhD Thesis, Universite de Toulouse

Jahromi A. S. and B. Bahr: An analytical method for predicting cutting forces in orthogonal machining of unidirectional composites. Compos. Sci. Technol., 70:1115–112, 2010.

Klinkova Olga, Joël Rech, Sylvain Drapier, and Jean-Michel Bergheau. 2011. “Characterization of Friction Properties at the Workmaterial/cutting Tool Interface during the Machining of Randomly Structured Carbon Fibers Reinforced Polymer with Carbide Tools under Dry Conditions.” Tribology International 44 (12): 2050–58.

Koplev A., Lystrup Aa., and Vorm T. 1983. “The Cutting Process, Chips, and Cutting Forces in Machining CFRP.” Composites 14 (4):371-76

Lasri L., M. Nouari, and M. El Mansori. 2009. “Modelling of Chip Separation in Machining Unidirectional FRP Composites by Stiffness Degradation Concept.” Composites Science and Technology 69 (5): 684–692.

Liu, DeFu, YongJun Tang, and W. L. Cong. 2012. “A Review of Mechanical Drilling for Composite Laminates.” Composite Structures 94 (4) : 1265–79.

Matzenmiller A., J. Lubliner et L. Taylor : A constitutive model for anisotropic damage in fiber-composites. Mechanics of materials, 20:125–152, 1995.

Merchant E: Mechanics of the metal cutting process. i. orthogonal cutting and type 2 chip. Journal of applied physics, 16:pp 267–275, 1945.

Nayak D., Bhantnagar N. and Mahajan P. 2005. "Machining Studies of Ud-Frp Composites Part 2: Finite Element Analysis." Machining Science and Technology 9 (4): 503-28

Pramanik A., L. C. Zhang, and J. A. Arsecularatne. 2007. "An FEM Investigation into the Behavior of Metal Matrix Composites: Tool–particle Interaction during Orthogonal Cutting." International Journal of Machine Tools and Manufacture 47 (10): 1497–1506.

Shchurov I. A., A. V. Nikonov, and I. S. Boldyrev. 2016. "SPH-Simulation of the Fiber-Reinforced Composite Workpiece Cutting for the Surface Quality Improvement." Procedia Engineering, 2nd International Conference on Industrial Engineering (ICIE-2016), 150: 860–65.

Wang X.M., and L Zhang. 2003. "An Experimental Investigation into the Orthogonal Cutting of Unidirectional Fibre Reinforced Plastics." International Journal of Machine Tools and Manufacture 43: 1015–22.

Zhang L. C., H. J. Zhang, and X. M. Wang. 2001. "A Force Prediction Model for Cutting Unidirectional Fibre-Reinforced Plastics." Machining Science and Technology 5 (3):293-305

Zitoune R., F. Collombet, F. Lachaud, R. Piquet, and P. Pasquet. 2005. "Experiment–calculation Comparison of the Cutting Conditions Representative of the Long Fiber Composite Drilling Phase." Composites Science and Technology, JNC13-AMAC-Strasbourg, 65 (3–4): 455–66.

Gadelmawla E S, Maksoud T.M.A., Elewa I.M., Soliman H.H., 2002. " Roughness parameters." Journal of Materials Processing Technology, 123: 133-145

Abaqus user manuel 2016 : http://abaqus.software.polimi.it/v2016/books/usb/default.htm?startat=pt04ch12s02aus84.html